

**NASA TECHNICAL NOTE**



**NASA TN D-4818**

*c.1*

**NASA TN D-4818**

LOAN COPY: R  
AFWL (W  
KIRTLAND AFI

0131502



TECH LIBRARY KAFB, NM

**THERMAL RADIATIVE AND ELECTRICAL  
PROPERTIES OF A CADMIUM SULFIDE  
SOLAR CELL AT LOW SOLAR  
INTENSITIES AND TEMPERATURES**

*by John R. Jack and Ernie W. Spisz*

*Lewis Research Center*

*Cleveland, Ohio*

TECH LIBRARY KAFB, NM



0131502

THERMAL RADIATIVE AND ELECTRICAL PROPERTIES OF A  
CADMIUM SULFIDE SOLAR CELL AT LOW SOLAR  
INTENSITIES AND TEMPERATURES

By John R. Jack and Ernie W. Spisz

Lewis Research Center  
Cleveland, Ohio

NATIONAL AERONAUTICS AND SPACE ADMINISTRATION

---

For sale by the Clearinghouse for Federal Scientific and Technical Information  
Springfield, Virginia 22151 - CFSTI price \$3.00

## ABSTRACT

A typical thin-film cadmium sulfide solar cell was investigated in a solar space environment simulator facility. The solar radiation intensity was varied from 0.028 to 1.07 solar constants. The associated solar-cell temperature ranged from 155 to 325 K. The results showed that the absorptance-emittance ratio was approximately constant at 0.43 over the temperature range of 200 to 325 K. Below 200 K the absorptance-emittance ratio increased rapidly to 0.70 at a temperature of 155 K.

THERMAL RADIATIVE AND ELECTRICAL PROPERTIES OF A  
CADMIUM SULFIDE SOLAR CELL AT LOW SOLAR  
INTENSITIES AND TEMPERATURES

by John R. Jack and Ernie W. Spisz

Lewis Research Center

SUMMARY

The ratio of solar absorptance to hemispherical emittance of a typical thin-film solar cell was determined for solar-cell temperatures ranging from 155 to 325 K. These temperatures correspond to simulated distances from the sun ranging from 5 to 0.97 astronomical units (AU). In addition, the cell electrical performance was determined experimentally for the same environmental conditions.

The results showed that the absorptance-emittance ratio was approximately constant at 0.43 over the temperature range 200 to 325 K. Below 200 K the absorptance-emittance ratio increased rapidly to 0.70 at a temperature of 155 K.

The cell electrical conversion efficiency optimized at 5 percent for a simulated distance from the sun of 3 AU. Open-circuit voltage increased from 325 to 520 millivolts, and short-circuit current decreased from 930 to 32 milliamperes as the distance from the sun increased from 1 to 5 AU.

INTRODUCTION

For some time, solar cells have been the dominant method of obtaining electrical power on long-life spacecraft. Their outstanding success can be attributed to their demonstrated long life and high degree of reliability on the many space missions flown. Consequently, it is expected that solar cells, of one type or another, will continue to be a primary source of space power for years to come.

It is recognized, however, that as space exploration horizons broaden, missions will be considered (ref. 1) with environments for which solar-cell performance is not known. Therefore, additional research is required on all cells. In particular, research is continuing on the relatively new thin-film cells, such as the cadmium sulfide cell,

because they are light in weight and flexible and offer the possibility of being launched and deployed in a simple, reliable fashion.

Many research areas involving thin-film solar cells are of interest and under investigation. For example, the effects of particle radiation and micrometeoroid impact on cell performance have been investigated at one solar constant (refs. 2 and 3). However, little has been done to obtain any cell performance for incident radiation conditions other than one solar constant ( $140 \text{ mW/cm}^2$ ). The important cell parameter, for radiation conditions other than one solar constant, is its temperature. The cell operating temperature is important because it influences both performance and durability. The operating temperature is governed by the energy balance of the cell, which, in turn, is primarily governed by the cell thermal radiative properties (solar absorptance and total hemispherical emittance). It is desirable, therefore, to determine the thermal radiative properties of thin-film cells so that the equilibrium temperature can be calculated for various space environments to which they may be exposed. Absorptances and emittances for thin-film cells are currently unavailable for the wide range of space conditions of interest.

This investigation was conducted to determine the ratio of solar absorptance to total hemispherical emittance of a typical cadmium sulfide solar cell. Values are presented for solar radiation intensities ranging from 0.028 to 1.02 solar constants with associated cell temperatures ranging from 155 to 328 K. In addition, the pertinent cell electrical characteristics were determined at equilibrium temperatures corresponding to radiation intensities of 0.04, 0.10, 0.54, and 1.07 solar constants.

## SYMBOLS

A	amplitude of temperature perturbation during cyclic period, K
$c_p$	specific heat, $\text{J}/(\text{g})(\text{k})$
$I_0$	radiant intensity, $\text{J}/(\text{cm}^2)(\text{sec})$
$I_1$	radiant intensity at 1 astronomical unit, $\text{J}/(\text{cm}^2)(\text{sec})$
$i_0$	intensity amplitude at mean temperature during cyclic equilibrium, $\text{J}/(\text{cm}^2)(\text{sec})$
k	intensity perturbation factor
m	solar-cell mass per unit area, $\text{g}/\text{cm}^2$
q	all heat-exchange terms other than those specified by remaining terms in equation (1), $\text{J}/(\text{cm}^2)(\text{sec})$
r	distance from sun, AU
T	solar-cell temperature, K

- $\dot{T}$  time rate of temperature change, K/sec
- $T_m$  mean cyclic temperature of cell, K
- $t$  time, sec
- $\alpha$  solar absorptance of front surface
- $\epsilon_b$  hemispherical emittance of back surface of cell
- $\epsilon_f$  hemispherical emittance of front surface of cell
- $\theta'$  time constant of material, sec
- $\sigma$  Stefan-Boltzmann constant,  $J/(cm^2)(sec)(K^4)$
- $\varphi$  phase angle between cell temperature and cyclic incident radiation, radians
- $\omega$  cyclic frequency, rad/sec

## THEORETICAL BACKGROUND

The method used herein to determine thermal radiative properties is described in detail in reference 4. The physical model consists of a thin sample (the solar cell) suspended in an ultra-high-vacuum, cold-wall environment. A radiant intensity  $I_0$  is imposed upon one surface of the sample to establish a sample equilibrium temperature  $T_m$ . The intensity is then perturbed sinusoidally with amplitude  $kI_0$  (where  $k < 1.0$ ) and frequency  $\omega$ .

The differential equation describing the temperature of an isothermal sample is, from reference 4,

$$mc_p \dot{T} = \alpha I_0 (1 + k \sin \omega t) + q - (\epsilon_f + \epsilon_b) \sigma T^4 \quad (1)$$

where  $\epsilon_f$  and  $\epsilon_b$  are the front- and back-surface emittance, respectively, and  $q$  contains all heat-exchange terms other than those specified by the remaining terms in equation (1).

Within the temperature range resulting from the intensity perturbation, the material properties ( $c_p$ ,  $\alpha$ ,  $\epsilon_f$  and  $\epsilon_b$ ) and the heat-exchange term  $q$  are considered to be independent of temperature. In addition, under these conditions the  $T^4$  term can be linearized about  $T_m$  as  $T^4 = 4T_m^3 T - 3T_m^4$ . With these assumptions, the solution of equation (1) is given by

$$T = T_m + A \left[ \sin (\omega t - \varphi) + e^{-t/\theta'} \sin \varphi \right] \quad (2)$$

The phase angle  $\varphi$  and amplitude  $A$  are related to the cell properties by

$$\varphi = \tan^{-1} \omega \theta' \quad (3)$$

and

$$A = \left( \frac{\alpha I_0 k}{mc_p} \right) \left[ \left( \frac{1}{\theta'} \right)^2 + \omega^2 \right]^{-1/2} \quad (4)$$

where  $\theta'$  is the time constant of the solar cell and is given by

$$\theta' = \frac{mc_p}{4(\epsilon_f + \epsilon_b)\sigma T_m^3} = \frac{1}{\omega} \tan \varphi \quad (5)$$

At cyclic equilibrium (i.e., when  $e^{-t/\theta'} \sin \varphi$  becomes negligible) the temperature response of the cell is sinusoidal around  $T_m$  with amplitude  $A$  and phase angle  $\varphi$ . Therefore, by measuring the phase angle  $\varphi$ , the frequency  $\omega$ , the temperature amplitude  $A$ , and the intensity perturbation amplitude  $kI_0$ , both the emittance and solar absorptance can be determined from equations (4) and (5), provided the specific-heat variation with temperature is known.

## APPARATUS AND PROCEDURE

### Environmental Facility

The application of the theory described in the preceding section requires a high-vacuum, cold-wall facility to eliminate residual gas conduction and to achieve low sample temperatures. Figure 1 is a schematic drawing of the high-vacuum facility and the experimental arrangement used. The facility is the Solar Space Environment Simulator Facility developed in 1960 at the Lewis Research Center and modified in 1966. The original oil diffusion and mechanical pumps have been replaced by liquid-nitrogen cryosorption pumps to eliminate oil backstreaming and possible contamination of the test surfaces. The facility is initially pumped to  $10^{-4}$  torr by the liquid-nitrogen cryosorption pumps. The annular wall of the test section and the baffles are then filled with liquid helium to cryopump the chamber below  $10^{-10}$  torr and also to provide a 4 K radiation background. The four liquid-helium-cooled baffles within the test section reduce stray radiation and permit the imposed collimated radiation to reach the model.

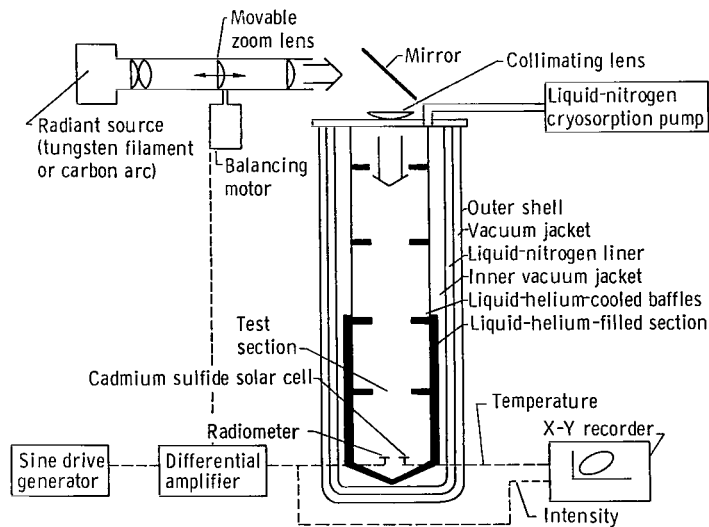


Figure 1. - Schematic drawing of environmental facility.

## Solar Cell and Mount

The solar cell used in this investigation is a current state-of-the-art 7.6- by 7.6-centimeter thin-film cadmium sulfide cell with a total area of 54.75 square centimeters. Its exact laminated construction is presented in table I along with the approximate thickness of each lamination. The composition and the fabrication of typical thin-film cadmium sulfide solar cells are discussed in detail in reference 5.

TABLE I. - THIN-FILM CADMIUM SULFIDE

### SOLAR-CELL CONSTRUCTION

[Total cell area, 54.75 cm<sup>2</sup>.]

Components (from front to back)	Approximate thickness, mm
Mylar	0.025
Epoxy cement	-----
Gold-plated copper grid	.010
Cuprous sulfide	<<.001
Cadmium sulfide	.025
Zinc	<<.001
Substrate of silver-filled, Pyre-ML coated on H-film	.050

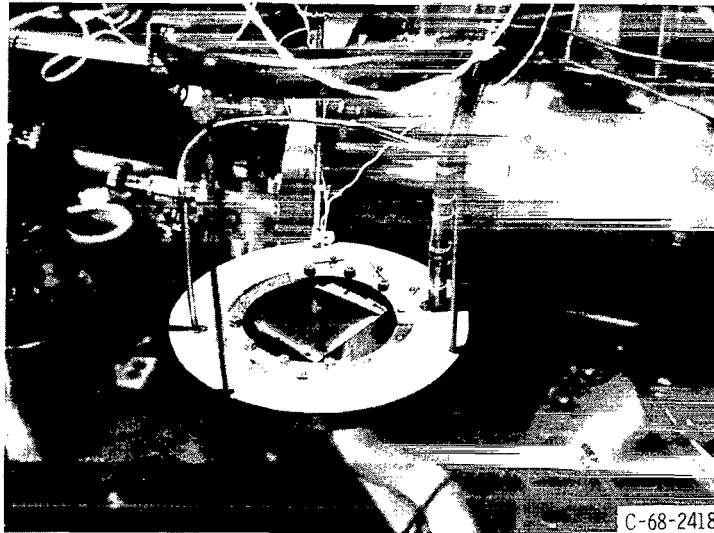


Figure 2. - Mounting of 7.6- by 7.6-centimeter cadmium sulfide solar cell.

The solar cell was mounted by suspending it in the environmental facility from four 26-gage copper wires fastened to the solar cell by an epoxy adhesive (fig. 2). The cell temperature was measured with a 36-gage copper-constantan thermocouple epoxied to the rear center of the cell. Small-diameter wires were used for the supports and the thermocouple to minimize their effect on the thermal response of the cell.

### Solar Simulator

The solar simulator consists of a 12-kilowatt carbon arc with associated collimating optics (fig. 1). The simulator output is a collimated beam with a maximum intensity of 250 milliwatts per square centimeter. Intensity can be continuously varied by the movable zoom lens to  $\pm 10$  percent of a given setting. Low intensity levels are obtained with the 12-kilowatt arc by using apertures and/or fine-wire mesh screens that act as neutral density filters (ref. 6). In addition a 1-kilowatt, quartz-iodine tungsten filament lamp can be substituted for the 12-kilowatt arc to provide stable, low-intensity radiation suitable for time-constant determinations.

Sinusoidal intensity perturbations are provided by automatic control of the movable zoom lens. The control system is composed of a calibrated silicon solar cell which is coupled with a reference sine generator into a differential amplifier that actuates a balancing motor to maintain the proper position of the zoom lens. The reference sine signal can be varied to produce both the desired amplitude and the cyclic frequency of the sinusoidal perturbation.

## Solar Simulator Spectral Distribution

The spectral energy distribution of the solar simulators was measured with a spectrometer. A transfer method of calibration was used over a wavelength range of 0.25 to 2.5 micrometers; that is, the spectrometer entrance slit was illuminated by a spectrally calibrated 1000-watt, quartz-iodine tungsten filament lamp whose calibration was traceable to an National Bureau of Standards (NBS) standard of spectral irradiance. Consequently, the spectral output of the "standard lamp" was determined as seen by the spectrometer. As a result, the spectrometer output does not resemble the standard-lamp spectral distribution because of spectral changes introduced by the spectrometer. For example, the mirror reflections, the prism transmittance, and the spectral response of the detector all change or influence the spectral output of the spectrometer. All these changes are combined into one factor defined as the spectrometer response. A spectrometer response curve is obtained by ratioing the spectrometer output to the spectral output of the standard lamp. Thus, the absolute spectral content of any source can be determined over a wavelength range of 0.25 to 2.5 micrometers with the spectral response curve obtained for the spectrometer.

The spectral distribution of the 12-kilowatt carbon arc solar simulator, obtained in the preceding manner, is compared in figure 3 with the Johnson curve (ref. 7). This comparison is based on making the radiant energy available from the carbon arc spectrum equal to that available from the Johnson spectrum over the wavelength interval 0.35 to 2.5 micrometers. Deviations of the carbon arc curve from the Johnson curve are small for the wavelength region of interest, 0.35 to 2.0 micrometers.

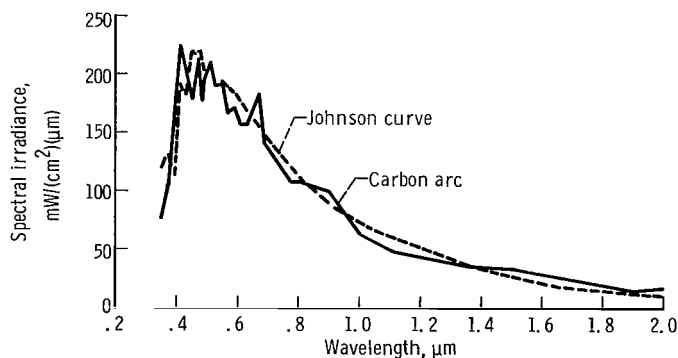


Figure 3. - Spectral irradiance of carbon arc solar simulator.

## Measurements and Accuracy

Data were recorded on a multichannel strip-chart recorder and an X-Y recorder. The strip-chart recorder monitors the radiant intensity and the solar-cell thermocouple to ensure the constancy of the absolute intensity level and frequency. The X-Y recorder is the primary data-recording instrument. A typical X-Y recorder trace over one cycle provides an elliptical Lissajous figure, such as that shown in figure 4. The reference sinusoidal intensity signal (or the calibrated solar-cell signal) is recorded on the x-axis and the cell temperature on the y-axis. The actual data trace is large with sufficient resolution to ensure accurate measurements of the mean sample temperature  $T_m$ , the amplitude of the temperature oscillation  $A$ , the initial intensity level  $I_0$ , and the amplitude of the intensity perturbation  $kI_0$ . From geometrical consideration of figure 4 (ref. 8) the phase angle between the cell temperature and the radiant intensity is given by

$$\varphi = \tan^{-1} \left[ \left( \frac{kI_0}{i_0} \right)^2 - 1 \right]^{1/2} \quad (6)$$

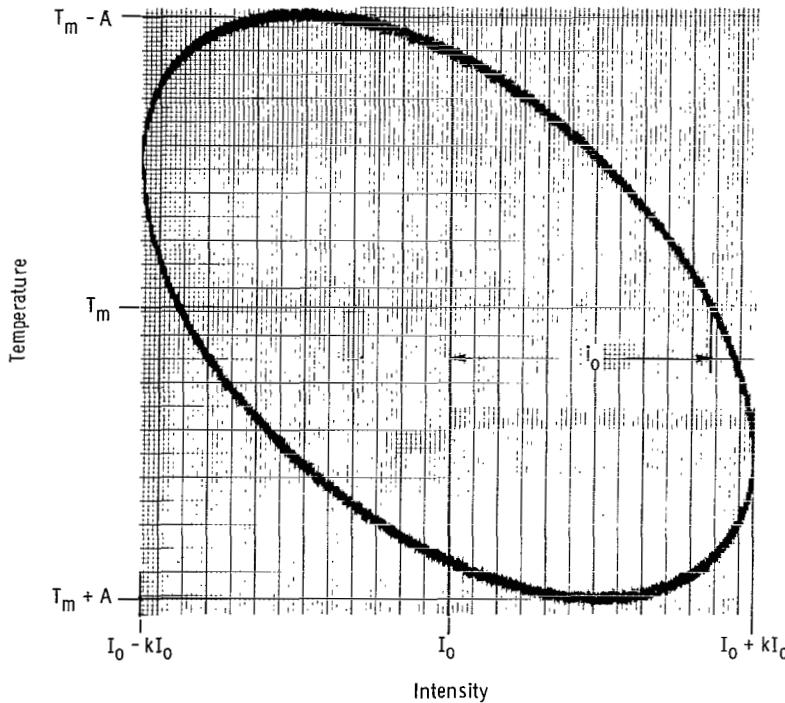


Figure 4. - Typical X-Y recorder trace.

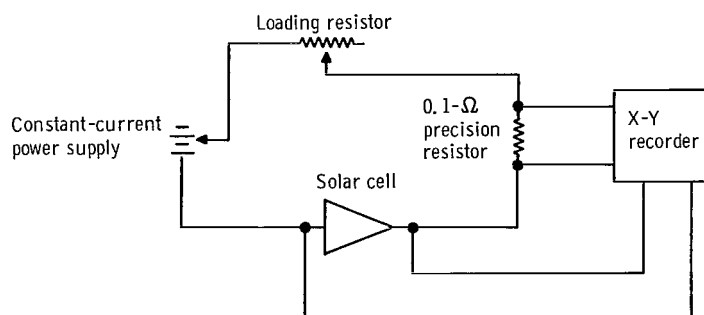


Figure 5. - Electrical circuit for determining electrical characteristics.

The Lissajous figure also provides an additional monitoring function on the experiment. The figure must close and repeat when cyclic equilibrium is achieved.

The voltage-current characteristics of the solar cell were obtained with the electrical circuit diagrammed in figure 5 and were recorded on an X-Y recorder. The electrical circuit consists of two separate loops, a high-impedance, zero-current loop for voltage measurement and a current-carrying loop for cell loading and current measurement. Cell loading was achieved through resistive loading or power-supply biasing.

Accuracy of the experimental data for thermal radiative properties was estimated from the uncertainties arising from the individual, basic measurements. The relative error of the absorptance-emittance ratio was determined from these uncertainties and calculated to be approximately  $\pm 5$  percent.

Measurement of the cell electrical properties was somewhat of a problem because the voltage and current fluctuated randomly about the steady value, especially at high currents. This fluctuation occurred because of the instabilities in the burning of the carbon arc. As a result, the electrical quantities presented herein are average values. Even so, the errors involved in the measured electrical properties are believed to be less than  $\pm 5$  percent.

## RESULTS AND DISCUSSION

### Thermal Radiative Properties

The thermal radiative properties of the cadmium sulfide cell were obtained at temperatures corresponding to radiant intensities that varied from 0.028 to 1.02 solar constants. The time constants (eq. (5)) as determined from the phase angles and imposed frequencies are shown in figure 6 as a function of cell temperature. The time constant

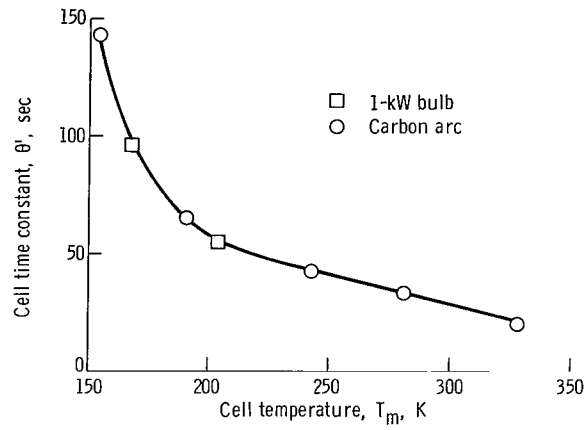


Figure 6. - Time constant of cadmium sulfide solar cell.

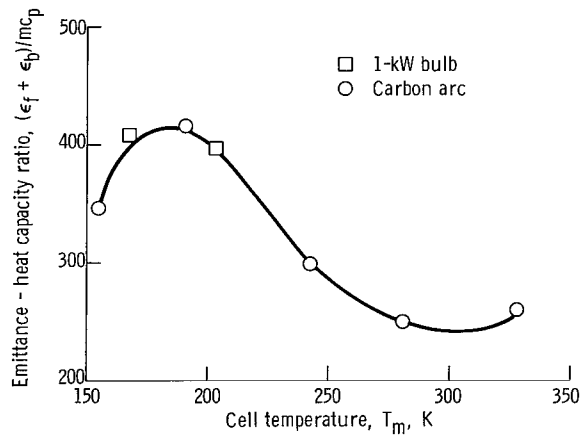


Figure 7. - Emittance of cadmium sulfide solar cell.

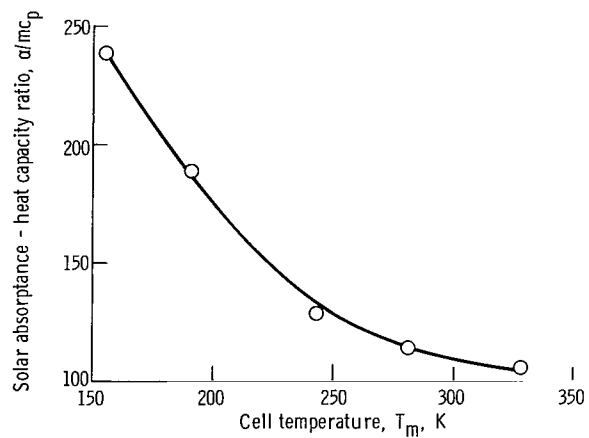


Figure 8. - Solar absorptance of cadmium sulfide solar cell (carbon arc source).

increases with decreasing temperature (eq. (5)), and the longest time constant obtained is 143 seconds at a cell temperature of 156 K. The longest time required to reach cyclic equilibrium is of the order of 12 minutes, approximately five times the time constant. Since this time is relatively short, there are no difficulties in meeting the critical requirement that all experimental parameters be held constant for this period.

Two data points obtained with the 1-kilowatt bulb are also included in figure 6 since the cell time constant is unaffected by the source spectral distribution. Data from the 1-kilowatt bulb should be more accurate than those obtained with the arc lamp because there are no instability problems. Nevertheless, all the time constants are consistent regardless of the source used.

In principle, with the time constants determined, the emittance can be found by using equation (5). Data from either the carbon arc or the 1-kilowatt bulb can be used to obtain emittance. Solar absorptances are obtained by substituting in equation (4) the additional measurements of temperature, amplitude  $A$ , and intensity amplitude  $kI_0$ . However, unlike the emittance determination, the 1-kilowatt-bulb data cannot be used in obtaining absorptance since the spectral distribution of the bulb is not comparable to that of the sun.

The emittance and absorptance data evaluated from equations (4) and (5) are presented in figures 7 and 8 in terms of the heat capacity per unit area of the cell. Presentation in this form was necessary because specific-heat data are not available for cadmium sulfide solar cells. However, the plots can be utilized to obtain absorptance and emittance when the specific-heat data become available as a function of temperature.

The important thermal radiative parameter that establishes the cell operating temperature is the absorptance-emittance ratio. This ratio can readily be obtained from the curves presented in figures 7 and 8. The absorptance-emittance ratio is shown in figure 9 for cell temperatures ranging from approximately 155 to 325 K. The important trend to note is the rapid decrease in the absorptance-emittance ratio  $\alpha/(\epsilon_f + \epsilon_b)$  as the temperature is increased. As the temperature increases from 155 to about 200 K, the absorptance-emittance ratio decreases from 0.70 to about 0.43, a decrease of 39 percent. A further increase in temperature beyond 200 K produces little change; the  $\alpha/(\epsilon_f + \epsilon_b)$  ratio remains approximately constant at a value of 0.43 to 325 K. Comparison of the 300 K experimental point presented in reference 9 with the preceding data shows good agreement.

For those interested in the mission aspects of the problem, the radiation intensity, cell equilibrium temperature, thermal radiative property data, and distance from the sun are all interrelated, in the ideal case, by the following equation:

$$(\epsilon_f + \epsilon_b)\sigma T^4 = \frac{\alpha I_1}{r^2} \quad (7)$$

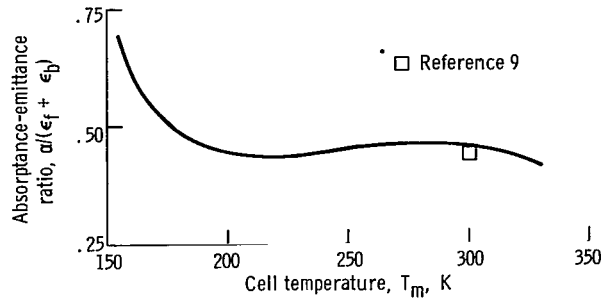


Figure 9. - Absorbance-emittance ratio for cadmium sulfide solar cell.

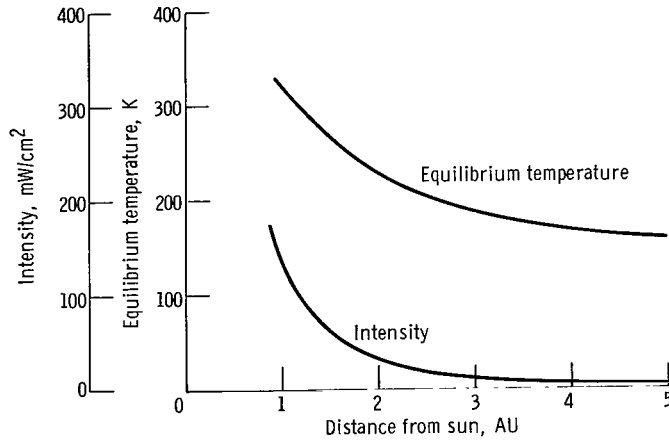


Figure 10. - Equilibrium temperature and solar radiation intensity at various distances from sun.

where  $I_1$  is the radiant intensity at 1 AU ( $140 \text{ mW/cm}^2$ ) and  $r$  is the distance from the sun in astronomical units. The calculated equivalent distances from the sun based on the measured variation of  $\alpha/(\epsilon_f + \epsilon_b)$  with equilibrium temperature are presented in figure 10. Equation (7) does not include the power produced by the solar cell. As a result, the equilibrium temperatures are slightly higher than would occur when the cell is generating power. Calculations indicate that, for a cell with an electrical conversion efficiency of 5 percent, the equilibrium cell temperature, while producing power, may be as much as 6 K lower than that presented herein.

From figures 9 and 10, the experimental absorbance-emittance ratios can be plotted as a function of equivalent distance from the sun. Results are shown in figure 11. This plot indicates that the absorbance-emittance ratio is approximately constant from 0.90 to 3 AU, or until an orbit approximately midway between Mars and Jupiter is reached. From there out into the solar system, the absorbance-emittance ratio apparently increases at a substantial rate.

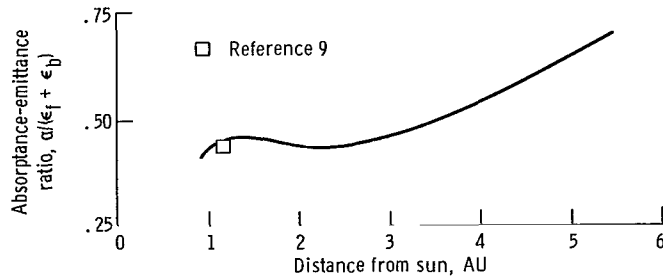


Figure 11. - Absorbance-emittance ratio of cadmium sulfide solar cell at various distances from sun.

## Electrical Properties

In addition to the thermal radiative properties of a cadmium sulfide solar cell, the electrical properties were also obtained under similar space conditions.

The cell electrical characteristics were measured for solar radiation varying from 0.04 to 1.07 solar constants and are presented in figure 12. The typical square characteristic was obtained for all values of solar radiation investigated. Short-circuit current, open-circuit voltage, and maximum electrical conversion efficiency  $\eta$

$$\eta = \frac{\text{Maximum electrical power}}{(\text{Cell area})(\text{Incident radiant intensity})}$$

were determined from the electrical characteristics and are presented in figure 13 as a function of distance from the sun. The short-circuit current behaves as anticipated, decreasing as the intensity of the solar radiation decreases. However, since open-circuit voltage and electrical conversion efficiency depend on both temperature and intensity, their behavior with distance from the sun cannot be easily predicted. The open-circuit voltage increases with increasing distance from the sun and becomes relatively constant at about 3 AU. This increase is due primarily to the decreasing cell operating temperature resulting from the decreasing radiant intensity (fig. 10). Figure 13 shows that the electrical efficiency first increases and then decreases at a slower rate as the distance from the sun is increased from 1 to 5 AU. An optimum efficiency of 5 percent is obtained at approximately 3 AU. This behavior occurs because the detrimental effect of reduced intensity overcomes the favorable effect of reduced cell temperature as the distance from the sun is increased. Therefore, to operate at maximum efficiency, cadmium sulfide solar-cell power supplies to be used for missions of less than 1 AU should include panel temperature control.

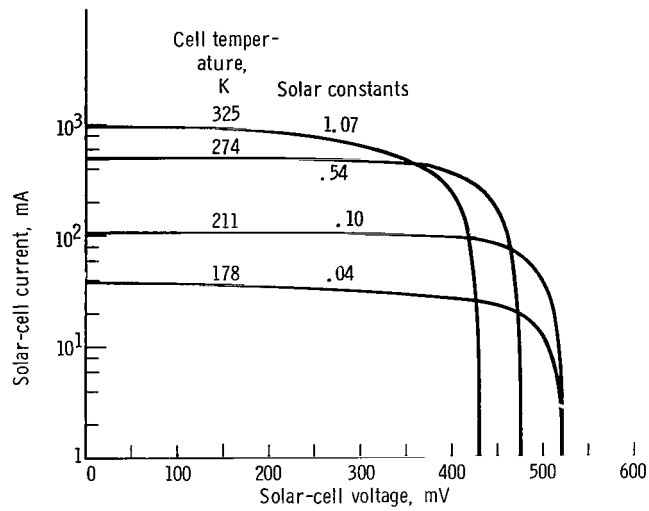


Figure 12. - Electrical characteristics of cadmium sulfide solar cell at various simulated solar radiation intensities.

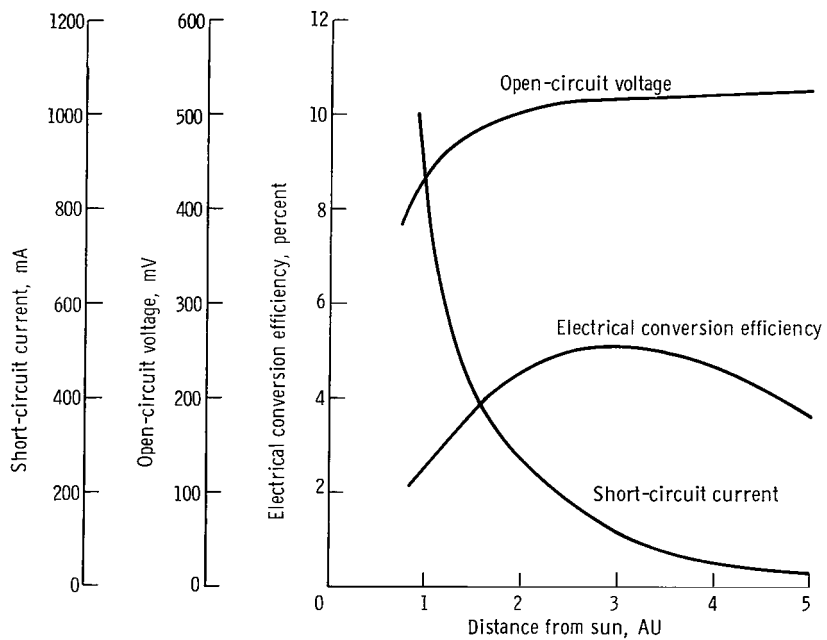


Figure 13. - Performance of cadmium sulfide solar cell at various distances from sun.

## SUMMARY OF RESULTS

Simulated space environmental tests were conducted on a current state-of-the-art thin-film cadmium sulfide solar cell to determine its thermal radiative and electrical properties. Solar radiation intensities were varied from 0.028 to 1.07 solar constants (5 to 0.97 astronomical unit (AU), respectively) with respective cell temperatures ranging from 155 to 325 K.

The absorptance-emittance ratio  $\alpha/(\epsilon_f + \epsilon_p)$  of the cell was approximately constant with a value of 0.43 over the temperature range from 200 to 325 K. Below 200 K, the  $\alpha/(\epsilon_f + \epsilon_p)$  ratio increased rapidly to 0.70 at a temperature of 155 K. The rapid increase may be due to a decrease in emittance below a temperature of 185 K.

The electrical efficiency of the cell at space equilibrium temperatures varied with equivalent distance from the sun. The electrical efficiency was 2.3 percent at 1 AU and 3.6 percent at 5 AU with a maximum efficiency of 5 percent at 3 AU.

Open-circuit voltage increased with increasing distance from 435 millivolts at 1 AU to 520 millivolts at 5 AU. This increase is due primarily to the decreasing temperature of the cell with decreasing radiant intensities. The short-circuit current of the cell decreased from 930 milliamperes at 1 AU to 38 milliamperes at 5 AU primarily because of the reduction in radiant intensity with increasing distance from the sun.

Lewis Research Center,  
National Aeronautics and Space Administration,  
Cleveland, Ohio, July 8, 1968,  
124-09-18-04-22.

## REFERENCES

1. Anon: OSSA Emphasizes Small-Scale Studies. Aviation Week & Space Tech., vol. 86, no. 26, 1967, p. 17.
2. Anon: Radiation Effects On Solar Cells and Photovoltaic Devices. Vol. I of the Proceedings of the Fourth Photovoltaic Specialists Conference. Rep. PIC-SOL-209/5, Pennsylvania Univ. (NASA CR-58680), Aug. 1964.
3. Mirtich, M. J.; and Bowman, R. L.: The Performance of N/P Silicon and CdS Solar Cells As Affected by Simulated Micrometeoroid Exposure. Radiation and Micrometeoroid Effects on Solar Cells, Lithium in Silicon Solar Cells. Vol. III of the Proceedings of the 6th Photovoltaic Specials Conference. IEEE, 1967, pp. 64-74.

4. Jack, John R. : Technique for Measuring Absorptance and Emittance by Using Cyclic Incident Radiation. *AIAA J.*, vol. 5, no. 9, Sept. 1967, pp. 1603-1606.
5. Shirland, F. A. ; and Augustine, F. : Thin Film Plastic Substrate CdS Solar Cells. Thin Film Solar Cells and Radiation Damage. Vol. II of Proceedings of the Fifth Photovoltaic Specialists Meeting. Rep. PIC-SOL-209/6.1, Pennsylvania Univ. (NASA CR-70169), Jan. 1966.
6. Heidt, Lawrence J. ; and Bosley, David E. : An Evaluation of Two Simple Methods For Calibrating Wavelength and Absorbance Scales of Modern Spectrophotometers. *J. Opt. Soc. Am.*, vol. 43, no. 9, Sept. 1953, pp. 760-766.
7. Johnson, Francis S. : The Solar Constant. *J. Meteorology*, vol. 11, no. 6, Dec. 1954, pp. 431-439.
8. Terman, Frederick E. ; and Pettit, Joseph M. : *Electronic Measurements*. Second ed., McGraw-Hill Book Co., Inc., 1952.
9. Liebert, Curt H. ; and Hibbard, Robert R. : Theoretical Temperatures of Thin-Film Solar Cells In Earth Orbit. NASA TN D-4331, 1968.

FIRST CLASS MAIL

68257 00903  
AERONAUTICAL ENGINEERING  
RESEARCH CENTER, MEXICO CITY, MEXICO

CONFIDENTIAL

POSTMASTER: If Undeliverable (Section 158  
Postal Manual) Do Not Return

*"The aeronautical and space activities of the United States shall be conducted so as to contribute . . . to the expansion of human knowledge of phenomena in the atmosphere and space. The Administration shall provide for the widest practicable and appropriate dissemination of information concerning its activities and the results thereof."*

— NATIONAL AERONAUTICS AND SPACE ACT OF 1958

## NASA SCIENTIFIC AND TECHNICAL PUBLICATIONS

**TECHNICAL REPORTS:** Scientific and technical information considered important, complete, and a lasting contribution to existing knowledge.

**TECHNICAL NOTES:** Information less broad in scope but nevertheless of importance as a contribution to existing knowledge.

**TECHNICAL MEMORANDUMS:** Information receiving limited distribution because of preliminary data, security classification, or other reasons.

**CONTRACTOR REPORTS:** Scientific and technical information generated under a NASA contract or grant and considered an important contribution to existing knowledge.

**TECHNICAL TRANSLATIONS:** Information published in a foreign language considered to merit NASA distribution in English.

**SPECIAL PUBLICATIONS:** Information derived from or of value to NASA activities. Publications include conference proceedings, monographs, data compilations, handbooks, sourcebooks, and special bibliographies.

**TECHNOLOGY UTILIZATION PUBLICATIONS:** Information on technology used by NASA that may be of particular interest in commercial and other non-aerospace applications. Publications include Tech Briefs, Technology Utilization Reports and Notes, and Technology Surveys.

*Details on the availability of these publications may be obtained from:*

SCIENTIFIC AND TECHNICAL INFORMATION DIVISION  
NATIONAL AERONAUTICS AND SPACE ADMINISTRATION  
Washington, D.C. 20546